

A Into-Plane Rotating Micromirror Actuated by a Hybrid Electrostatic Driving Structure *

Wu Wengang¹, Chen Qinghua¹, Yin Dongqing², Yan Guizhen¹,
Chen Zhangyuan², Hao Yilong¹, and Xu Anshi²

(1 National Key Laboratory of Micro/ Nano Fabrication Technology, Institute of Microelectronics,
Peking University, Beijing 100871, China)

(2 National Laboratory on Local Fiber-Optic Communication Networks & Advanced Optical Communication Systems,
Department of Electronics, Peking University, Beijing 100871, China)

Abstract : A novel into-plane rotating micromirror actuated by a hybrid electrostatic driving structure is presented. The hybrid driving structure is made up of a planar plate drive and a vertical comb drive. The device is fabricated in SOI substrate by using a bulk-and-surface mixed silicon micromachining process. As demonstrated by experiment ,the novel driving structure can actuate the mirror to achieve large-range continuous rotation as well as spontaneous 90° rotation induced by the pull-in effect. The continuous rotating range of the micromirror is increased to about 46° at an increased yielding voltage. The measured yielding voltages of the mirrors with torsional springs of 1 and 0.5μm in thickness are 390 ~ 410V and 140 ~ 160V ,respectively. The optical insertion loss has also been measured to be - 1.98dB when the mirror serves as an optical switch.

Key words : micromirror ; hybrid electrostatic driving structure ; planar plate drive ; vertical comb drive ; mixed silicon micromachining

EEACC : 2575 ; 4145 ; 2560Z **PACC :** 4283 ; 0710C

CLC number : TN389 **Document code :** A **Article ID :** 0253-4177(2005)09-1699-06

1 Introduction

MEMS (micro-electromechanical systems) is a key technology for many kinds of new actuators such as micromirrors. Actuated micromirrors can provide optical switching^[1,2], scanning, projecting^[3], modulating^[4], and attenuating^[5] functions by steering reflected light in an analog or digital control fashion for wide-ranging various applications such as fiber networking, sensing, imaging, data collection, and optical adaptation. As a result, MEMS-based micromirrors especially in an array

format have received much attention over the past few years.

Most of the torsional micromirrors reported to date employed electrostatic drives to achieve rotation into, or out of, the wafer plane. The electrostatic drives exhibit several major advantages including low power consumption, simple structures, and are hence easy to fabricate^[6,7]. The previously reported electrostatic drives for torsional micromirrors include planar plate drives (PPDs) and vertical comb drives (VCDs)^[8-10]. The PPDs consist of two planar plates and have been used to achieve 90° rotation^[11-13] based on the pull-in effect^[10]. The pull-in

* Project supported by the National Natural Science Foundation of China (No. 60278028) and the State Technology Innovation Program of Beijing City (No. 772167384624)

Wu Wengang male, professor. His current researches are on micro-electromechanical systems (MEMS) and nano-electromechanical systems (NEMS), etc.

Chen Qinghua male, PhD candidate. He mainly focuses on research about optical MEMS.

Received 8 April 2005

© 2005 Chinese Institute of Electronics

effect, however, limits the continuous rotating range of the mirrors. And the largest continuous rotating range so far demonstrated is within 30° by both theoretical modeling and experimentation^[11,13].

The VCDs, on the other hand, consist of two sets of comb fingers, and one is movable and the other is fixed. The movable and fixed comb fingers are uneven and interdigitated. The VCDs can offer the mirrors a continuous and stable rotation over the entire operating range due to the lack of pull-in effect. They also generate a higher force density, leading to large deflections of the mirrors at low voltages^[14]. However, the VCDs can not make 90° rotation.

This article reports on a hybrid electrostatic drive that integrates a PPD and VCD in the same structure for actuating torsional micromirrors. In the current structure, the VCD section is used to create large-range continuous rotation, and the PPD section is used to create spontaneous 90° rotation induced by the pull-in effect. As demonstrated by experiment, the fabricated devices can achieve continuous rotation up to about 46° . However, accompanying the increase in the continuous rotating range, the yielding voltage^[11,13] increases.

2 Design and fabrication

2.1 Structure

Figure 1 is the three-dimensional (3D) schematic structure of the present micromirror actuated by a hybrid electrostatic driving structure. The micromirror with comb fingers is suspended by an elastic torsional spring across a rectangular through-cavity. The mirror can rotate with the torsional spring as the pivot.

The hybrid driving structure includes a PPD and VCD. The PPD consists of the mirror and a sidewall. The torsional spring is parallel with and very near to the sidewall. In the mirror-sidewall drive (MSD), the sidewall is used to attract the mirror electrically, and to stop its rotating movement as it has rotated by 90° . The VCD consists of

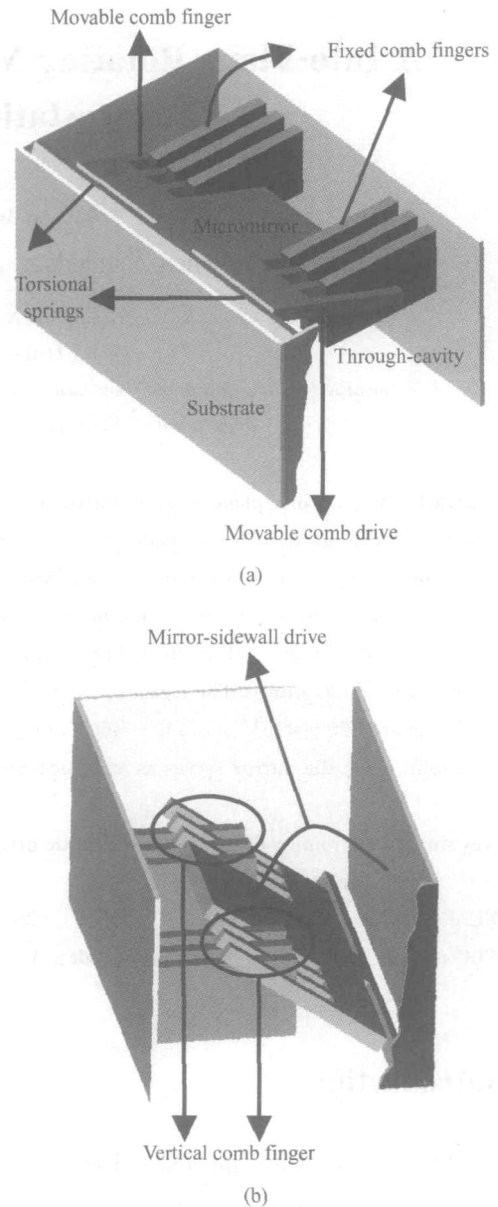


Fig. 1 3D schematic structure of the torsional micromirror actuated by a hybrid electrostatic driving structure (a) Front side view of the mirror with a rotation angle; (b) Backside view of the mirror with a rotation angle

a set of movable comb fingers and a set of fixed comb fingers. The movable comb fingers are located symmetrically on both sides of the mirror, and will move together with the mirror. The fixed comb fingers are located on the other sidewall parallel with the torsional spring, formed by using the same etching steps for producing the cavity itself. The two sets of comb fingers become interdigitated as the movar-

ble comb fingers rotate with the mirror.

In the hybrid driving structure ,the VCD performs the function of increasing the threshold deflection ,in other word increasing the continuous rotating range of the mirror. The MSD plays the role of inducing the pull-in effect ,thus the spontaneous 90 ° rotation at a larger threshold deflection.

2.2 Fabrication

A set of bulk-and-surface mixed silicon micromachining process has been developed to fabricate the present device in SOI substrate. Figure 2 schematically depicts the sequence of the main steps of the fabrication process. With an SiO₂ film deposited and then patterned as a mask, the micromirror with movable comb fingers was produced in the single crystal silicon device layer by using KOH wet etch and then inductively-coupled-plasma (ICP) dry etch. After another SiO₂ film had been deposited as protection layer for the mirror surface, a composite-mask composed of an inner SiO₂ and an outer sputtered Al layer was produced on the backside of the SOI substrate. The silicon handle layer was milled anisotropically from the back by using ICP etch to partially form the cavity ,the fixed comb fingers on one sidewall of the cavity ,and the fiber grooves. A sandwich layer consisting of SiO₂/ Si₃N₄/ SiO₂ was deposited ,and then

removed from the device and electrode regions on the SOI substrate. Sputtering and then patterning Au/ Cr on the top surface was followed to produce electrodes ,and to further improve optical reflectivity of the mirror as well as electric conductivity. A portion of the SiO₂/ Si₃N₄/ SiO₂ sandwich layer on the backside was etched in an anisotropic reactive ion etching (RIE) step ,leaving the other part on the sidewalls of the cavity ,the fixed comb fingers , and the grooves unaffected. Then ,the cavity and fixed comb finger structure were etched from the back with ICP till the SiO₂ box of the SOI substrate interrupts the etching. At the same time ,the handle layer in the groove regions was also further etched. Finally ,the SiO₂ box also served as a sacrificial layer was removed to release the micromirror with movable comb fingers after the silicon handle layer had been isotropically etched slightly more from the back. The mirror with comb fingers became fully suspended by the elastic torsional spring over the through-cavity. In fact ,during the last structure-releasing step ,the outside SiO₂ sublayer in the SiO₂/ Si₃N₄/ SiO₂ sandwich layer on the sidewalls of the cavity ,the fixed comb fingers ,and the grooves was also removed. However ,its Si₃N₄ and inside SiO₂ sublayers were maintained to serve as an insulating film ,e. g. ,between the mirror having rotated by 90 °and the stopper sidewall.

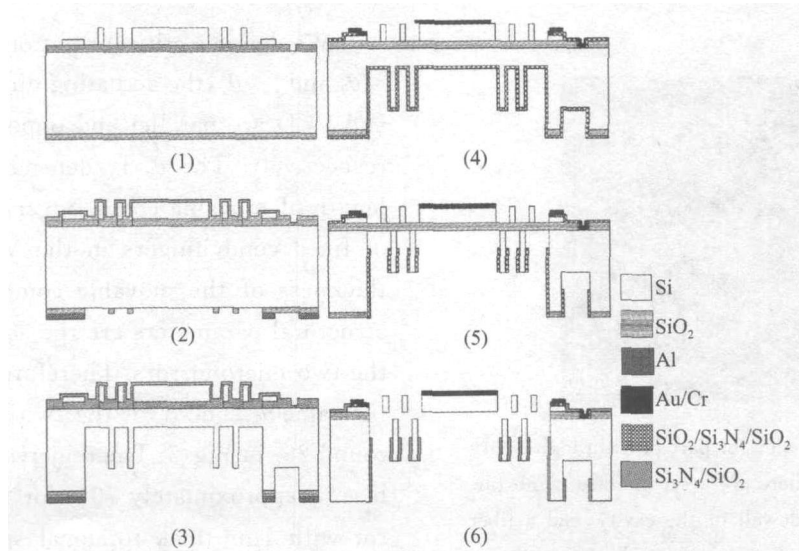


Fig.2 Schematic sequence of the main steps of the bulk-and-surface mixed silicon micromachining process for fabricating the present device in SOI substrate

In order to decrease actuation voltage, the elastic torsional springs were fabricated thinner than the micromirrors. The thicknesses of the mirrors are 5 and 2 μm depending on the SOI substrates used, with the corresponding thicknesses of the elastic torsional springs being 1 and 0.5 μm , respectively. By using well-controlled ICP etch, 380 μm -deep through-cavities and fixed comb fingers with a depth up to 180 μm were obtained, with their sidewalls being perpendicular to the SOI substrate plane. Figure 3 illustrates the scanning electron microscope (SEM) image of one of the manufactured micromirrors. Figure 4 shows the backside SEM view of part of a through-cavity with fiber grooves. As can be seen, a set of fixed comb fingers and a fiber holding structure are located on one sidewall of the cavity and on one sidewall of a groove, respectively.

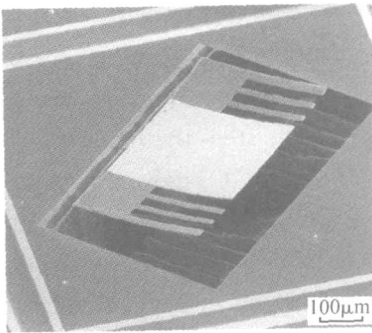


Fig. 3 SEM image of one fabricated torsional micromirror

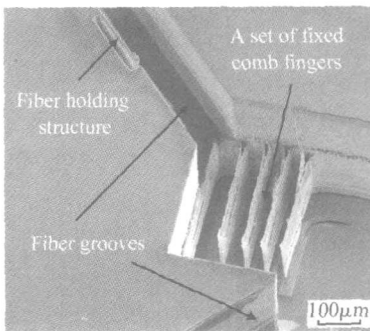


Fig. 4 Backside SEM view of part of a through-cavity with fiber grooves. There are a set of fixed comb fingers formed on one sidewall of the cavity, and a fiber holding structure formed on one sidewall of a groove.

3 Experimental characterization

When a DC bias is applied between one of the torsional micromirrors and the handle layer of SOI substrate, the mirror is driven electrically and rotates into its through-cavity. The DC bias dependence of the rotation angle of the mirrors was observed in an atmospheric pressure with a laser reflecting system. Figure 5 depicts the measured θ -bias curves of two fabricated mirrors, which are a 5 μm -thick mirror with 1 μm -thick torsional spring, and a 2 μm -thick mirror with 0.5 μm -thick torsional spring. In the hybrid electrostatic driving structures of the two mirrors, the MSDs are the same, whereas the VCDs have minor differences.

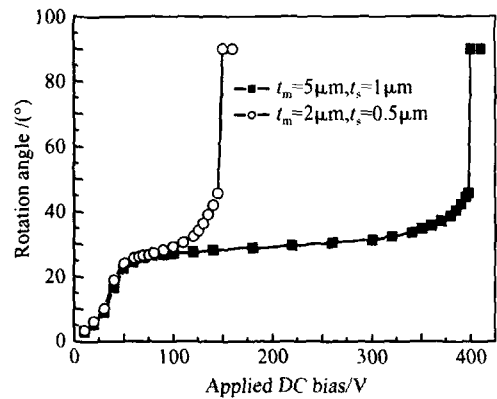


Fig. 5 Experimental characteristic of mirror rotation angle versus applied DC bias

We define a critical rotation angle θ_0 as: when $\theta < \theta_0$ and $\theta > \theta_0$, the actuating directions of the MSD and VCD are parallel and opposite to each other, respectively. The θ_0 is dependent mainly on the length of movable comb fingers and the thickness of fixed comb fingers in the VCD^[15]. Except the thickness of the movable comb fingers, all other structural parameters are the same in the VCDs of the two micromirrors. Therefore, they have almost the same θ_0 . The θ_0 of the two mirrors is found around 26° in Fig. 5. The θ_0 increases to θ_0 under the bias of approximately 70V for the 5 μm -thick mirror with 1 μm -thick torsional spring, and approximately 60V for the 2 μm -thick mirror with 0.5 μm -thick torsional spring, respectively. When θ begins

to be larger than θ_0 , the increase of θ with the bias increasing becomes relatively slow.

When the applied DC bias is increased to the value slightly higher than the electrostatic yielding voltages, the pull-in effect takes place, and subsequently, the mirrors rotate to 90° spontaneously till they touch the stopper sidewalls within the cavities^[11,13], as indicated in Fig. 5. The measurement results of the yielding voltages for the $5\mu\text{m}$ -thick mirror with $1\mu\text{m}$ -thick torsional spring and the $2\mu\text{m}$ -thick mirror with $0.5\mu\text{m}$ -thick torsional spring are $390 \sim 410\text{V}$ and $140 \sim 160\text{V}$, respectively, depending on the measured samples. As a comparison, the typical electrostatic yielding voltages of conventional micromirrors actuated only by MSDs are found to be $270 \sim 290\text{V}$ for $1\mu\text{m}$ -thick torsional springs^[13] and $100 \sim 150\text{V}$ for $0.4\mu\text{m}$ -thick torsional springs^[11], respectively.

The measurement values of the threshold deflections are about 46° . The threshold deflection of the $5\mu\text{m}$ -thick mirror with $1\mu\text{m}$ -thick torsional spring is not specifically equal to that of the $2\mu\text{m}$ -thick mirror with $0.5\mu\text{m}$ -thick torsional spring, but the difference between them is minimal. As a comparison, the typical threshold deflections of the conventional torsional micromirrors are found to be approximately 30° ^[11,13]. Therefore, compared with the conventional mirrors, the continuous rotating range of the present one is increased from 30° to 46° .

Figure 5 manifests that the hybrid electrostatic driving structure can actuate the mirror to achieve not only large-range continuous rotation but also spontaneous 90° rotation induced by the pull-in effect, which will in turn be very useful when both functions are necessary for certain applications. However, there exists a trade-off between the continuous rotating range and the yielding voltage. Accompanying the increase in the continuous rotating range, the yielding voltage increases.

The insertion loss in the optical coupling system consisting of the mirror, input and output fiber ends, where the torsional micromirror is used as an

optical switch, has also been investigated through experimentation. The switch is in ON-state when the mirror has rotated by 90° . The schematic measurement system is shown in Fig. 6. Standard single mode fibers with special rod lenses were used as the input and output fibers to reduce the light diffraction from input fiber end, and simultaneously enhance the light collection into the output fiber end. The incident light beam from the input fiber, which exhibits a central wavelength of 1550nm and small diffraction, is introduced to the mirror having rotated by 90° through the free space in a fiber groove illustrated in Fig. 4. Reflected by the mirror, the beam transmits out through the free space in another fiber groove and is collected then by the output fiber. The obtained insertion loss is -1.98dB . In addition, the reflectivity of the micromirror was also measured to be $92.3\% \sim 95.5\%$.

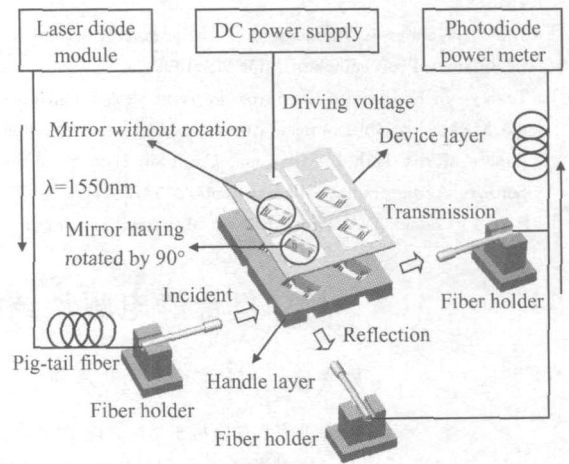


Fig. 6 Schematic experimental system for measuring the optical insertion loss when the mirrors serve as optical switches

4 Conclusion

In summary, a novel into-plane rotating micromirror actuated by a hybrid electrostatic driving structure has been demonstrated. The device is fabricated in SOI substrate based on bulk-and-surface mixed silicon micromachining. Measurements indicate that not only large-range continuous rotation but also spontaneous 90° rotation induced by the

pull-in effect can be achieved for the mirror, and the continuous rotating range is increased to approximately 46° . However, as a trade-off of the increase in the continuous rotating range, the yielding voltage increases. Experimental observation also demonstrates that the optical insertion loss can reach approximately -1.98dB when the mirror is used as an optical switch.

References

- [1] Liang Chunguang, Xu Yongqing, Yang Yongjun. Fabrication of MEMS optical switches. Chinese Journal of Semiconductors, 2001, 22(12): 1551 (in Chinese) [梁春广, 徐永青, 杨拥军. MEMS 光开关. 半导体学报, 2001, 22(12): 1551]
- [2] Wu Wengang, Hao Yilong, Li Dachao, et al. Fabrication and electromechanical characteristics of 2×2 torsion-mirror optical switch arrays with monolithically integrated fiber self-holding structures. Chinese Journal of Semiconductors, 2002, 23(10): 1024
- [3] Kessel P F V, Hornbeck L J, Meier R E, et al. A MEMS-based projection display. Proceedings of the IEEE, 1998, 86(8): 1687
- [4] Dür P, Gehner A, Dauderstädt U. Micromirror spatial light modulators. Proceedings of MOEMS, 1999: 60
- [5] Toshiyoshi H, Isamoto K, Morosawa A, et al. A 5-volt operated MEMS variable optical attenuator. Digest of Technical Papers of the 12th International Conference on Solid-State Sensors, Actuators and Microsystems, 2003, 2: 1768
- [6] Bart S F, Lober T A, Howe R T, et al. Design considerations for micromachined electric actuators. Sensors and Actuators, 1988, 14: 269
- [7] Trimmer W S N, Gabriel K J. Design considerations for a practical electrostatic micro-motor. Sensors and Actuators, 1987, 11: 189
- [8] Yeh J L A, Jiang H, Tien N C. Integrated polysilicon and DRIE bulk silicon micromachining for an electrostatic torsional actuator. J Microelectromech Syst, 1999, 8(4): 456
- [9] Selvakumar A, Najafi K. Vertical comb array microactuators. J Microelectromech Syst, 2003, 12(4): 440
- [10] Hah D, Huang S, Nguyen H, et al. Low voltage MEMS analog micromirror arrays with hidden vertical comb-drive actuators. Technical Digest of the Solid-State Sensor, Actuator and Microsystems Workshop, 2002: 11
- [11] Toshiyoshi H, Fujita H. Electrostatic micro torsion mirrors for an optical switch matrix. J Microelectromech Syst, 1996, 5(4): 231
- [12] Yoon Y S, Bae K D, Kim J H, et al. A low voltage actuated micromirror with an extra vertical electrode for 90° rotation. Journal of Micromechanics and Microengineering, 2003, 13(6): 922
- [13] Wu W G, Li D C, Sun W, et al. Fabrication and characterization of torsion mirror actuators for optical networking applications. Sensors and Actuators A, 2003, 108(1-3): 175
- [14] Hagelin P M, Krishnamoorthy U, Heritage J P, et al. Scalable optical cross-connect switch using micromachined mirror. IEEE Photonics Technol Lett, 2000, 12(7): 882
- [15] Patterson P R, Hah D, Nguyen H, et al. A scanning micromirror with angular comb drive actuation. Technical Digest of the 15th International Conference on Micro Electro Mechanical Systems, 2002: 544

复合静电驱动结构致动的内旋转微镜*

吴文刚¹ 陈庆华¹ 尹冬青² 闫桂珍¹ 陈章渊² 郝一龙¹ 徐安士²

(1 北京大学微电子学研究院 微米/纳米加工技术国家级重点实验室, 北京 100871)

(2 北京大学电子学系 区域光纤通信网与新型光纤系统国家重点实验室, 北京 100871)

摘要: 报道了以体硅表面硅混合微加工工艺制作在 SOI 衬底上的一种新型复合静电驱动结构致动内旋转微镜, 其中复合静电驱动结构由一个平板驱动器和一个垂直梳齿驱动器构成. 实验表明, 该新型驱动结构不仅能使微镜实现大范围连续旋转, 而且能使微镜实现吸合效应致自发性 90° 旋转. 微镜的连续旋转范围扩大到约 46° , 同时引发吸合效应的拐点电压也增大. 对于具有 1 和 $0.5\mu\text{m}$ 厚扭转弹性梁的微镜, 实测拐点电压分别为 $390 \sim 410\text{V}$ 和 $140 \sim 160\text{V}$. 当该微镜用作光开关时, 测得光插入损耗为 -1.98dB .

关键词: 微镜; 复合静电驱动结构; 平板驱动器; 垂直梳齿驱动器; 硅混合微加工

EEACC: 2575; 4145; 2560Z **PACC:** 4283; 0710C

中图分类号: TN389 **文献标识码:** A **文章编号:** 0253-4177(2005)09-1699-06

*国家自然科学基金(批准号:60278028)和北京市国家技术创新计划(批准号:772167384624)资助项目

吴文刚 男, 教授, 目前主要研究方向为 MEMS/ NEMS.

陈庆华 男, 博士研究生, 主要从事光学 MEMS 的研究.

2005-04-08 收到